We are IntechOpen,
the world's leading publisher of
Open Access books
Built by scientists, for scientists

4,800
Open access books available

122,000
International authors and editors

135M
Downloads

Our authors are among the

154
Countries delivered to

TOP 1%
most cited scientists

12.2%
Contributors from top 500 universities

CLARIVATE ANALYTICS
BOOK CITATION INDEX
INDEXED

WEB OF SCIENCE™

Selection of our books indexed in the Book Citation Index
in Web of Science™ Core Collection (BKCI)

Interested in publishing with us?
Contact book.department@intechopen.com

Numbers displayed above are based on latest data collected.
For more information visit www.intechopen.com

Modeling of Dielectric Resonator Antennas using Numerical Methods Applied to EPR

Sounik Kiran Kumar Dash and Taimoor Khan

Additional information is available at the end of the chapter

Abstract

This chapter presents an inclusive analysis of notable techniques carried out on modeling of dielectric resonator (DR)-antenna using numerical methods in last more than two decades. Dielectric resonator antenna (DRA) has created its individual existence in antenna engineering because of its captivating characteristics like; small size, low loss, high efficiency, wide bandwidth, three-dimensional design flexibility as compared to conventional antennas, etc. The DR antennas are being widely modeled using numerical methods nowadays. The triple-folded intention of this chapter is to: (1) give an overview on DRA modeling using single and hybrid numerical methods, (2) give a compressive review of notable numerical modeling researches carried out on DRAs and (3) give some favorable future concentration for the antenna researchers in order to apply the numerical methods on some innovative geometries of DRAs.

Keywords: antennas, dielectric resonator antennas, electromagnetics, microwave, numerical modeling

1. Introduction

The term DR (dielectric resonator)-antenna or some time DRA (dielectric resonator antenna) is derived from dielectric, resonator, and antenna, simultaneously. It is basically an antenna in which a dielectric material resonates at a certain frequency. The word dielectric resonator (DR) was firstly used by Richtmyer [1] long back in mid-1939s. The idea of using DR as a radiating element i.e. antenna in cylindrical shape had been firstly accepted in mid-1983s [2]. DR-antennas have several interesting advantages like; small size, large power handling capacity, less dissipation loss, high efficiency, compatible to any 3-D shape, etc. which make them more popular than that of the traditional antennas. The power handling capability, less loss, and

high efficiency are mainly because of the low loss tangent and permittivity of the dielectric resonator while the three-dimensional design flexibility is the function of number of controlling parameters of the resonator's fundamental shapes like; radius for hemispherical shape, height to radius ratio for cylindrical shape and depth/width as well as length/width ratio for rectangular shape [3]. However, because of the advanced simulation and mechanical tools available, different shapes like; hollow cylindrical, conical, hexagonal, triangular, etc. shapes as shown in **Figure 1** are available nowadays.

The mathematical methods used for modeling of DRAs are broadly classified as analytical methods and numerical methods. Up to 1940, the classical methods were widely used for solving the narrow range of electromagnetic (EM) problems only because of complex geometries and mathematical complexities. However, in the mid-1960s, due to the availability of relatively high speed computers, the numerical methods have been supported in their implementation to the EM problems [4]. Since then, numerical methods have taken the place of analytical methods due to numerous advantages, like; lesser computational time, economic for labor purpose, etc. The proposed chapter describes only the three numerical methods: FDTD (finite difference time domain), FEM (finite element method), and MOM (method of moment) which are being widely used for DRAs modeling. In context to this, here different researches carried out on numerical modeling of DRAs in last more than two decades are disused.

2. Dielectric resonator and its antenna characteristics

The gradual development of modern communication systems from microwave-to-millimeter wave had given a chance to Long et al. [2] to investigate dielectric resonator (DR) as a radiator, as a better solution to avoid unnecessary radiation loss, conduction loss, and lower efficiency of conventional microstrip/waveguide antennas at higher frequencies. In course of time, the applications of DRs are not limited to only millimeter but are widely used in microwave and radio frequency ranges also now-a-days. This is because of its several attractive physical characteristics, like 3D-design flexibility, high/low Q-factor, light weight, low cost, ease of excitation, etc. as well as several improved performances in terms of bandwidth, gain, etc. as discussed in the previous section.

Initially, the dielectric resonator was invented in the form of a high Q-factor element specifically used for filters and oscillators [1]. Because of the high Q-factor, the amount of energy stored was much more than the amount of energy lost, which made it to be used as an energy storage device. Once the Q-factor is low, the working is vice versa i.e. the energy radiated is much higher than the energy stored [1]. As per Long et al. [2], when a DR (of low Q-factor) is
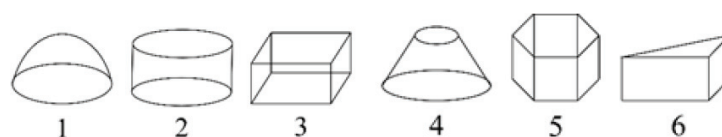
Figure 1. Different geometrical shapes of DR antennas (1—hemispherical, 2—cylindrical, 3—rectangular, 4—conical, 5—hexagonal, and 6—triangular).

placed on a metallic ground surface with unshielded surroundings and an excitation is applied to it, then the discontinuity of the relative permittivity at the resonator surfaces plays an important role. It enables the radio waves bounce back and forth in between the resonator boundary and called as standing electromagnetic wave, means it resonates as well as creates chances of reflection but cannot radiate. It is well known that the resonator walls designed to be transparent to radio waves. Once, the resonator is excited at proper resonating mode, the radio waves start penetrating the resonator boundary and radiate into space. The desired resonating mode can be achieved by proper positioning of dielectric resonator, ground plane, feed, and slot. Moreover, the field distribution inside the resonator as well as the radiation pattern in the space, are distinct depending upon the resonating mode at which the resonator is excited. These modes are mainly divided into three different modes, like transverse electric (TE), transverse magnetic (TM), and hybrid electromagnetic (HEM) modes [3–4]. Generally, for rectangular DRAs, the fundamental modes are considered to be TE_{x111}, TE_{y111}, and TE_{z111}, respectively. For hemispherical DRAs, these are considered as TE_{111} and TM_{101}. Similarly, for cylindrical DRAs, these modes are considered as TE_{01}, TM_{01}, and HE_{11}/EH_{11} [3, 4].

3. FDTD modeling of DRAs

The Finite-Difference-Time-Domain method is one of the popular methods in context of electromagnetic scattering. From historical point of view; the finite difference time domain method was first developed by Yee in 1966 [5]. Later on, it has been extended to electromagnetic three dimensional cases with steady state excitation and also considered to be one of the feasible alternatives to those frequency domain methods. Apart from this, FDTD method has been recognized to be one of the most effective numerical methods in the study of metamaterial-based structures. In 1990, this FDTD method became one of the popular methods of choice for electromagnetic problem analysis, because of several advantages like: ease of understanding, short development time, and explicit type nature [6]. This method has been successfully implemented in different electromagnetic problems like; scattering of antenna (microstrip patch antenna, dielectric resonator antenna), microstrip circuits, etc. However, for the convenience of the readers, few general steps of using FDTD method for DRA modeling are further illustrated in this section.

3.1. Few general steps for FDTD implementation on DRAs

Generally the FDTD method is formulated by considering the differential form of Maxwell's two curl equations which describe the propagation of electric as well as magnetic fields in any medium, which can be uniform, homogeneous, and isotropic. In addition to this, the medium is assumed to be lossless i.e., null volume currents or finite conductivity. Thus, the Maxwell's curl equations can be written as described:

$$\mu \frac{\partial H}{\partial t} = -\nabla \times E \text{ and } \varepsilon \frac{\partial E}{\partial t} = \nabla \times H \tag{1}$$

Here $\mu = \mu_0 \mu_r$ and $\varepsilon = \varepsilon_0 \varepsilon_r$.

For the solution of this type of partial differential equation by FDTD method, a first order finite difference scheme can be used for both time as well as space.

3.2. Step 1: field in time and spatial domain

Let us consider a three dimensional problem as shown in **Figure 2** and define the electric field (or magnetic field) in both space and time domain as [7]:

$$\frac{\partial F(x,y,z,t)}{\partial x} \approx \frac{(F(x+\Delta x/2,y,z,t)-F(x-\Delta x/2,y,z,t))}{\Delta x} = \frac{(F^n(i+0.5,j,k)-F^n(i-0.5,j,k))}{\Delta x}$$

(2)

$$\frac{\partial F(x,y,z,t)}{\partial t} \approx \frac{(F(x,y,z,t+\Delta t/2)-F(x,y,z,t-\Delta t/2))}{\Delta t} = \frac{(F^{n+0.5}(i,j,k)-F^{n-0.5}(i,j,k))}{\Delta t}$$

(3)

As the field is discretized in both space and time domain, hence the practical calculation space is also divided into number of small cubes as shown in **Figure 2(a)**. Here each small cube $\Delta x \times \Delta y \times \Delta z$ of the problem is known as cell size.

3.3. Step 2: Yee's algorithm

For a three-dimensional case, the six field locations are considered as interleaved in space as shown in **Figure 2(b)**. Here each small cells are known as FDTD unit cell [5]. The E-field is calculated at each midpoint of small FDTD cell and for convenience purpose the H-field can be calculated at each spatial locations between two adjacent E-fields.

The field component of x-direction can be written as;

$$H_x^{n+0.5}(i+1,j+0.5,k+0.5) = H_x^{n-0.5}(i+1,j+0.5,k+0.5)$$

$$+\frac{\Delta t}{\mu}\left(\frac{E_y^n(i+1,j+0.5,k+1)-E_y^n(i+1,j+0.5,k)}{\Delta z} - \frac{E_z^n(i+1,j+1,k+0.5)-E_z^n(i+1,j,k+0.5)}{\Delta y}\right)$$

(4)
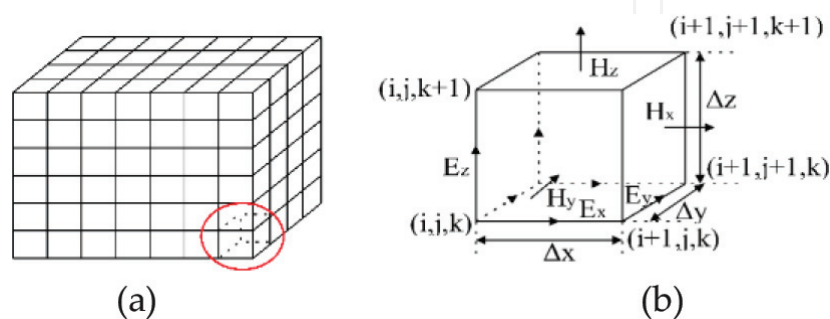
Figure 2. FDTD analysis [7]. (a) FDTD lattice and (b) unit cell.

$$E_x^{n+1}(i+0.5,j,k) = E_x^n(i+0.5,j,k)$$

$$+ \frac{\Delta t}{\varepsilon} \left(\frac{H_z^{n+0.5}(i+0.5,j+0.5,k) - H_z^{n+0.5}(i+0.5,j-0.5,k)}{\Delta y} - \frac{H_z^{n+0.5}(i+0.5,j,k+0.5) - H_z^{n+0.5}(i+0.5,j,k+0.5)}{\Delta z} \right)$$

$$(5)$$

Similarly, the field components for y- and z-direction for both electric and magnetic fields can be easily determined. It should be noted here that if the E-field is calculated at nΔt, the H-field is calculated at (n + 0.5)Δt, for which Yee's algorithm is also known as leapfrog algorithm.

3.4. Step 3: estimation of cell size and time step

It is obvious that in FDTD method, finer cell is taken by assuming constant field over a cell. However, the size of the cell depends upon the wavelength of the material. Smaller cell size gives better accuracy. In case of high permittivity dielectric material, the non-homogeneous type cell-size can be used. After fixing the cell-size, the time step can be taken as per Courant-Fricdrich-Lewy stability condition [13].

$$\Delta t \leq \frac{1}{v_{\max}} \left(\frac{1}{\Delta x^2} + \frac{1}{\Delta y^2} + \frac{1}{\Delta z^2} \right)^{-1/2} \qquad (6)$$

Here $V_{\max}$ is the maximum phase velocity of the wave in the computational domain/volume. This equation ensures that, error generated in one step does not increase with time marching and using this condition the grid dispersion error can be minimized.

3.5. Step 4: dielectric resonator antenna analysis

A DR-antenna can be a three-dimensional dielectric geometry of any shape along with conducting feed and ground plane. The FDTD method assumes perfect conductor approxima-tion for microstrip line/patch/ground plane whereas perfect dielectric approximation for sub-strate as well as dielectric resonators. In FDTD modeling, the fundamental parameters like; permittivity, permeability, and conductivity are assigned to respective cells in the computa-tional domain to form the objects. Microstrip line/patch/ground plane are generally considered as two-diemensional geometry. Hence the tangential E-field component must be null (0) on the surface. Thus, it can be modeled by applying the boundary conditions on the respective planes of the proper cells. Then, the non-perfect conductor cells like: substrate, dielectric resonator or air, are assigned with respective permittivity (ε_r). For air ε_r will be unity, for substrate and DR the permittivity (ε_r) value can be taken as per the modeling requirement. But for a stacking case, the average value of the interfaces of two/multi dielectric constant can be assigned [7].

3.6. Step 5: source signal and feed modeling

For excitation of the dielectric resonator, the different waveforms like: plane wave, modulated pulse, etc. can be applied. However, in view of smooth waveform, the Gaussian pulse type excitation is preferably used which is mentioned in Eq. (7).

$$p(t) = \begin{cases} e^{-\left[\frac{(t-t_0)}{T_s}\right]^2} & 0 \le t \le 2t_0 \\ 0 & Otherwise \end{cases} \tag{7}$$

where T_s = spread time, t_0 = peak time.

In practical case, signal is given to the feed line through SMA connector. This feeding in FDTD approach can be modeled by assigning several electric area within the area along the thickness/ height of the substrate which just comes under the strip. Then if the pulse is generated, the fields in the three-dimensional structure can be computed for successive steps until the steady state arrives. Thus, the input impedance (Z_{in}) of the dielectric resonator antenna is calculated easily using Eq. (8)

$$Z_{in}(f) = \frac{V_s(f)}{I_s(f)} \tag{8}$$

where, $V_s(f)$ and $I_s(f)$ are the Fast Fourier Transform (FFT) of the time domain source voltage and source current respectively. Then the return loss can be calculated as:

$$RL_{dB}(f) = 20 \log \left(\frac{Z_{in}(f) - Z_0}{Z_{in}(f) + Z_0} \right) \tag{9}$$

Here Z_0 = 50 Ohm.

3.7. Step 6: boundary conditions

During the analysis of EM problems, it is necessary to truncate the computational domain by a virtual boundary. In addition to this, the boundary should be absorbing one in order to absorb all the radiation to avoid reflection which may causes errors. Hence, it is termed as absorbing boundary condition (ABC) which can be of either Mur's ABC [8] or Berenger's Perfectly Matched Layer (PML) [9]. However, PML is best ABC in terms of accuracy [7].

The above basic steps shows the advancement in computational electromagnetics using FDTD which enabled many researchers for modeling several complex problems based on DRAs. Some notable researches carried out based on this approach in last decade are discussed here.

In 1994, Shum and Luk [10] have analyzed a rectangular DR-antenna fed by a microstrip line through an aperture made on ground plane using FDTD method for calculating the return losses. Again, [11] have analyzed dielectric ring resonator antenna with an air-gap using the FDTD method for improving the impedance bandwidth of the antenna by adjusting the air-gap spacing. A cylindrical dielectric antenna with a dielectric coating has been analyzed using FDTD method for observing the effect of the relative permittivity of the coating material on the impedance bandwidth of the antenna. Then, again [12] have analyzed a cylindrical DRA operating at the fundamental broadside mode using FDTD method for observing the impact of the feed position, probe length, and the dielectric constant on input impedance. Shum and

Luk [13] have presented a FDTD numerical method for modeling probe-fed cylindrical DR antenna for computing the input impedance of the antenna operating in $HEM_{11\delta}$ mode. Chen et al. [14] have analyzed a probe-fed section-spherical DRA using FDTD technique. The mutual coupling between aperture-coupled cylindrical DRAs has been analyzed using FDTD [15]. The aperture-coupled CDRA on a thick ground plane has been investigated using the FDTD method for reducing the coupling from feed-line to the antenna by increasing the thickness of the ground plane [16]. A cross-shaped DRA designed for circular polarization has been analyzed via conformal FDTD method [17]. Kamchouchi and Kayar [18] have demonstrated FDTD method for simplifying the sophisticated radiation problems. Semouchkina et al. [19] have used FDTD method to study the resonant modes in DR-antenna. The in detail study of inter-element coupling phenomena based on a FDTD technique utilizing Berenger's PML boundary conditions and geometrical symmetries has been presented by Gentili et al. [20]. A Microstrip-slot coupled rectangular DRA operated in fundamental TE_{111} mode has been investigated numerically and experimentally [21]. Top-hat monopole antennas loaded with radial layered dielectric has been analyzed using FDTD method for computing input impedance of the antenna structure more accurately [22]. Zhang et al. [23] have investigated a probe-fed DRA element operating in a waveguide environment with application to spatial power combining amplifier arrays using FDTD technique. The radiation pattern and input impedance of the strip-fed rectangular shaped DRA have been computed numerically using FDTD method [24]. Nomura and Sato [25] have proposed a combined method of topology optimization and FDTD method for wideband DR-antenna design. Mohanana et al. [26] have investigated a microstrip line excited compact rectangular DRA using FDTD method. FDTD method has been used to calculate the input impedance of the cylindrical DR-antenna with different dimensions [27]. Li et al. [28] have studied a differentially fed RDRA using FDTD method for the fundamental TE_{111} mode at 2.4 GHz, with a bandwidth of 10.4%. Li and Leung [29] have analyzed a differentially fed rectangular DRA using FDTD method. Thus, the several cases of DRAs have been described using FDTD in this section. Yao et al. [30] have presented an efficient two-dimensional FDTD method for analyzing the parallel-plate dielectric resonator. A Pawn DRA has been investigated in time domain for predicting about 122% impedance bandwidth [31]. Dzulkipli et al. [32] have used a simulation technique based on FDTD to analyze mutual coupling effects in reflectarray environment. Gupta and Gangwar [33] have presented numerical analysis of input impedance, return loss, and radiation characteristics of a strip excited triangular shape DRA (TDRA) using FDTD technique. Thus, several cases based on different shapes of DR-antennas have been successfully resolved.

4. Method of moments for DRAs modeling

Method of moments is sometimes known as moment method (MM). It is considered to be the oldest method in terms of deriving point estimators. The name "method moments" is mainly originated from Russian literature. In western literature, the method of moments has been firstly attributed by Harrington [34], however it became much popular in electromagnetic modeling after the work by Harrington [35]. In course of time MOM has been successfully

applied to several practical EM problems like radiation caused by thin-wire elements and arrays, scattering problems, analysis of microstrip and lossy structures and later on for DRA also. So in this context, the modeling of dielectric resonator antenna with some basic steps is clearly discussed in this section. Moreover some published articles of DRA modeling based on this method is also summarized here.

4.1. Few general steps for MOM implementation on DRAs

The integral equations (IE) techniques are quite effective in providing exact solution for dielectric structure modeling. During the modeling of homogeneous system, the integral equations (IE) can be expressed in terms of tangential component of fields (both electric and magnetic) at the media interface only. The equivalence principle [36] is normally used for the solution of scattering problem by using MoM.

4.2. Step 1: representation of field(s) in terms of θ and φ

Magnetic field and electric field can be expressed in term of scalar and vector potential by considering position r in θ and ϕ direction for three-dimensional problem as [37]:

$$E_r = \frac{1}{j\omega\varepsilon\mu}\left(\frac{\partial^2}{\partial r^2} + k^2\right)A_r \tag{10}$$

$$E_\theta = \frac{-1}{\varepsilon r \sin\theta}\cdot\frac{\partial F_r}{\partial\phi} + \frac{1}{j\omega\varepsilon\mu r}\cdot\frac{\partial^2 A_r}{\partial r\partial\theta} \tag{11}$$

$$E_\phi = \frac{1}{\varepsilon r}\cdot\frac{\partial F_r}{\partial\theta} + \frac{1}{j\omega\varepsilon\mu r\sin\theta}\cdot\frac{\partial^2 A_r}{\partial r\partial\phi} \tag{12}$$

$$H_r = \frac{1}{j\omega\varepsilon\mu}\left(\frac{\partial^2}{\partial r^2} + k^2\right)F_r \tag{13}$$

$$H_\theta = \frac{1}{\mu r \sin\theta}\cdot\frac{\partial A_r}{\partial\phi} + \frac{1}{j\omega\varepsilon\mu r}\cdot\frac{\partial^2 F_r}{\partial r\partial\theta} \tag{14}$$

$$H_\phi = \frac{-1}{\mu r}\cdot\frac{\partial A_r}{\partial\theta} + \frac{1}{j\omega\varepsilon\mu r\sin\theta}\cdot\frac{\partial^2 F_r}{\partial r\partial\phi} \tag{15}$$

4.3. Step 2: formulation of electric and magnetic potential using Green's function

The electric potential due to a point current J_θ inside and outside the dielectric resonators can be expressed as:

For inside DR (i.e. r < a):

$$G_{J_\theta}^{F_r} = \sum_{n=0}^{\infty} \sum_{m=-n}^{n} A_{nm} P_n^m (\cos\theta) e^{jm\phi} \hat{J}_n(kr) \tag{16}$$

$$G_{J_\theta}^{A_r} = \sum_{n=0}^{\infty} \sum_{m=-n}^{n} B_{nm} P_n^m (\cos\theta) e^{jm\phi} \hat{J}_n(kr) \tag{17}$$

For outside DR (i.e. r > a):

$$G_{J_\theta}^{F_r} = \sum_{n=0}^{\infty} \sum_{m=-n}^{n} C_{nm} P_n^m (\cos\theta) e^{jm\phi} \hat{H}_n(k_0 r) \tag{18}$$

$$G_{J_\theta}^{A_r} = \sum_{n=0}^{\infty} \sum_{m=-n}^{n} D_{nm} P_n^m (\cos\theta) e^{jm\phi} \hat{H}_n(k_0 r) \tag{19}$$

Here the $G_{J_\beta}^{F_r}$ and $G_{J_\beta}^{A_r}$ are the electric potential and magnetic potential in β directed point current, respectively whereas β can be either θ or ϕ. $P_n^m(\cos\theta)$: related to Legendre function of order m and degree n. $\hat{J}_n(kr)$ and $\hat{H}_n(k_0 r)$ represents the spherical Bessel functions of the first kind and spherical Hankel function of the second kind respectively. A_{nm}, B_{nm}, C_{nm}, and D_{nm} can be determined from the boundary condition at the DR-air interface (i.e. r = a) (**Figure 3**).

After applying the boundary condition $E_\theta^+ - E_\theta^- = 0$ as well as $E_\phi^+ - E_\phi^- = 0$ for E-field and $H_\theta^+ - H_\theta^- = 0$ as well as $H_\phi^+ - H_\phi^- = -J_\theta$ ($-J_\theta$ is taken by considering the θ directed current) for H-filed at (r = r′ = a) for both θ and ϕ direction four sets of equation relating A_{nm}, B_{nm}, C_{nm}, and D_{nm} can be established, like Eq. (20) (for E-field) and Eq. (21) (for H-field) [37]:

$$\pm K X_{nm} \hat{J}_n(ka) \pm K Y_{nm} \hat{H}_n(k_0 a) = 0 \tag{20}$$

$$\pm K X_{nm} \hat{J}_n(ka) \pm K Y_{nm} \hat{H}_n(k_0 a) = 1 \tag{21}$$

where $\hat{j}_n(ka)$ and $\hat{k}_n(k_0 a)$ are the spherical Bessel function and spherical Henkel function, respectively, K is the ratio of wave number and permittivity, and X_{nm}, Y_{nm} are either A_{nm}, C_{nm} or B_{nm}, D_{nm} [37]. Out of the four sets of equation, by combing the TE mode equations (which
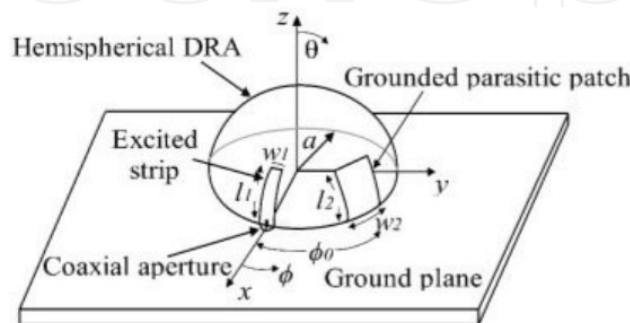
Figure 3. Analysis of hemipsherical DRA [37].

relate to A_{nm}, C_{nm} (in E-field) and B_{nm}, D_{nm} (in H-field)) and TM-mode equation (which relate to B_{nm}, D_{nm} (in E-field) and A_{nm}, C_{nm} (in H-field)) can give a straight forward solution for all four unknowns i.e. A_{nm}, B_{nm}, C_{nm}, and D_{nm}. By putting these values in equation (16-19), the simplified versions of Green's function $G_{J_\theta}^{F_r}$ and $G_{J_\theta}^{A_r}$ can be obtained for both inside (r < a) and outside (r > a) region. Again by applying the similar procedure, the Green's function $G_{J_\phi}^{F_r}$ and $G_{J_\phi}^{A_r}$ for φ directed current can also be obtained.

4.4. Step 3: formulation of E-field and H-field using Green's function

The total E-field because of θ directed and φ directed point currents can be found from potential Green's function. By substituting the values of $G_{J_\theta}^{F_r}$ and $G_{J_\theta}^{A_r}$ (for inside as well as outside cases) in Eqs. (10-15), it can be obtained [37]:

$$
\begin{aligned}
G_{J_\theta}^{E_\theta} = \frac{j\eta_0}{2\pi a r} \sum_{n=0}^{\infty} \frac{2n+1}{n(n+1)} \sum_{m=0}^{n} \frac{(n-m)!}{(n+m)!} \cos m(\phi - \phi') \\
\times \left\{ \frac{m^2}{\Delta_n^{TE}} \frac{P_n^m(\cos\theta')}{\sin\theta'} \frac{P_n^m(\cos\theta)}{\sin\theta} \Phi_n - \frac{1}{\Delta_n^{TM}\Delta_m} \frac{d}{d\theta} P_n^m(\cos\theta)\psi_n \right\}
\end{aligned}
\tag{22}
$$

Like this $G_{J_\theta}^{E_\phi}$, $G_{J_\phi}^{E_\theta}$ and $G_{J_\phi}^{E_\theta}$ can be obtained [37]. The function Φ_n and ψ_n have different forms for E-field inside (r < a) and outside (r > a) of the dielectric resonator (**Figure 3**). Then with Green's function for the solution of the current (either in the feed probe/feed line/patch/strip etc.) can be found/solved by using MoM.

4.5. Step 4: solution of current using MoM

This Method of Moment solution can be well understood by taking an example (as shown in **Figure 3**). Let in this figure the β (either θ or ϕ) directed E-field ${}^A E_{J_\theta}^\beta$, ${}^B E_{J_\theta}^\beta$, ${}^B E_{J_\phi}^\beta$ are produced by θ directed excitation strip current J_θ^A, patch current J_θ^B and φ directed patch current J_ϕ^B respectively. Now, by imposing the boundary condition, so that total E-field must vanish on the conducting excitation strip, we get;

$$
{}^A E_{J_\theta}^\theta + {}^B E_{J_\theta}^\theta + {}^B E_{J_\phi}^\theta + E^i = 0
\tag{23}
$$

Which can be expressed in terms of Green's functions, i.e.

$$
\iint_{S_A} G_{J_\theta}^{E_\theta} J_\theta^A dS' + \iint_{S_B} G_{J_\theta}^{E_\theta} J_\theta^B dS' + \iint_{S_B} G_{J_\phi}^{E_\theta} J_\phi^B dS' + {}^A E^i = 0
\tag{24}
$$

Here, S_A and S_B are the surfaces of the excitation strip and parasitic patch respectively, which can further be expressed as:

$$\frac{-1}{W_1} \iint_{S_A} G_{J_\theta}^{E_\theta} I_\theta^A dS' + \frac{-1}{W_2} \iint_{S_B} G_{J_\theta}^{E_\theta} I_\theta^B dS' + \frac{-1}{L_2} \iint_{S_B} G_{J_\phi}^{E_\theta} I_\phi^B dS' = \frac{1}{a}\delta(\theta) \tag{25}$$

Here: $^A E^i = (V_0/a)\delta(\theta)$ and $V_0 = 1$ (unity).

$I_\theta^A = J_\theta^A W_1$, $I_\theta^B = J_\theta^B W_2$, and $I_\phi^B = J_\phi^B L_2$.

Now these currents can be expanded using MoM and resulted as:

$$I_\theta^A(\theta) = \sum_{p_1=1}^{N_1} I_{p_1}^{\theta A} f_{p_1}^{\theta A}(\theta) \tag{26}$$

$$I_\theta^B(\theta) = \sum_{p_2=1}^{N_2} I_{p_2}^{\theta B} f_{p_2}^{\theta B}(\theta) \tag{27}$$

$$I_\phi^B(\theta) = \sum_{p_3=1}^{N_3} I_{p_3}^{\phi B} f_{p_3}^{\phi B}(\phi) \tag{28}$$

where, $f_{p_1}^{\theta A}(\theta)$, $f_{p_2}^{\theta B}(\theta)$, and $f_{p_3}^{\phi B}(\phi)$ are PWS basis functions [38]. Similarly two more equations can be obtained by enforcing the boundary conditions, like;

$$^A E_{J_\theta}^\theta + {}^B E_{J_\theta}^\theta + {}^B E_{J_\phi}^\theta = 0 \tag{29}$$

$$^A E_{J_\theta}^\phi + {}^B E_{J_\theta}^\phi + {}^B E_{J_\phi}^\phi = 0 \tag{30}$$

By applying Galerkin's procedure again we can obtain three sets of equations as of Eqs. (26)–(28). Then the whole equation set can be solved by using the following matrix formulation [4]:

$$\begin{bmatrix} \left[Z_{\theta\theta}^{AA'}(p_1,q_1)\right]_{N_1 \times N_1} & \left[Z_{\theta\theta}^{AB'}(p_1,q_2)\right]_{N_1 \times N_2} & \left[Z_{\theta\phi}^{AB'}(p_1,q_3)\right]_{N_1 \times N_3} \\ \left[Z_{\theta\theta}^{BA'}(p_2,q_1)\right]_{N_2 \times N_1} & \left[Z_{\theta\theta}^{BB'}(p_2,q_2)\right]_{N_2 \times N_2} & \left[Z_{\theta\phi}^{BB'}(p_2,q_3)\right]_{N_2 \times N_3} \\ \left[Z_{\phi\theta}^{BA'}(p_3,q_1)\right]_{N_3 \times N_1} & \left[Z_{\phi\theta}^{BB'}(p_3,q_2)\right]_{N_3 \times N_2} & \left[Z_{\phi\phi}^{BB'}(p_3,q_3)\right]_{N_3 \times N_3} \end{bmatrix} \times \begin{bmatrix} \left[I_{p_1}^{\theta A}\right]_{N_1 \times 1} \\ \left[I_{p_2}^{\theta B}\right]_{N_2 \times 1} \\ \left[I_{p_3}^{\phi B}\right]_{N_3 \times 1} \end{bmatrix} = \begin{bmatrix} \left[V_{q_1}^{A}\right]_{N_1 \times 1} \\ [0]_{N_2 \times 1} \\ [0]_{N_3 \times 1} \end{bmatrix} \tag{31}$$

After the current vector $\left[I_{p_1}^{\theta A}\right]$ is obtained from Eq. (31), the input impedance can easily be calculated from $Z_{in} = \gamma/\sum_{p_1=1}^{N_1} I_{p_1}^{\theta A} f_{p_1}^{\theta A}(0)$. Further, here $\gamma = 1$ for equivalent spherical DR while 0.5 for hemispherical DR. Then, the remaining current vectors $\left[I_{p_2}^{\theta B}\right]$, $\left[I_{p_3}^{\phi B}\right]$ together along with $\left[I_{p_1}^{\theta A}\right]$ can be used to calculate the radiation fields of dielectric resonator antenna. Thus, few general mathematical steps are discussed here for implementation of method of moments

which are quite useful and simple. The use of this method for analyzing some DRAs in last decades is further summarized here.

Analysis of the disk antennas above the grounded dielectric substrate has been carried out using moment method [39]. The input impedance of a cylindrical DRA excited by an aperture slot has been computed using MOM method together with an efficient matrix solution algorithm [40]. Leung and Luk [41] have studied an aperture-coupled hemispherical DRA using MM method for broadside TE_{111} mode. An aperture-coupled hemispherical shaped DR-antenna operating at the end-fire TE_{221} mode has been studied using MOM method together with Green's function [42]. Liu et al. [43] have analyzed a DRA based on the electric and magnetic field integral equations using MM method. The Green function technique together with the MM method has been used to determine the equivalent magnetic current in the slot of slot-fed DRA with/without a backing cavity [44]. Kishk et al. [45] have done a numerical study of split cylindrical DRAs on a conducting ground plane excited by a coaxial probe excited in HEM_{11} and HEM_{12} modes based on MM method. Then MOM-based surface integral equation solver for studying arbitrarily shaped aperture coupled DRAs has been developed [46]. Chow and Leung [47] have investigated the input impedance of the cavity-backed slot-coupled DRA excited by a slender strip using the MM method. The MOM method with piecewise sinusoidal (PWS) basis and testing functions has been used for analyzing a circularly polarized DRA excited by a spiral slot [48]. A rigorous analysis has been done for the excitation of hemispherical type DR-antenna loaded by a circular disk using MOM [49]. Baghaee et al. [50] have analyzed a probe-fed rectangular DRA on a finite ground plane using MOM. A rigorous analysis of the slot-coupled hemispherical dielectric resonator top-loaded by a conducting cap has been presented using MOM [51]. Eshrah et al. [52] have proposed excitation of DRAs by waveguide slots as a substitute to traditionally used excitation mechanism as well as to enhance bandwidth and to control the power coupled to the DRA using MOM method. The coaxial-aperture-fed hemispherical DRA has been analyzed using MOM method [53]. Lam and Leung [54] have analyzed U-slot excited DRA with a baking cavity using the MOM. Ge and Esselle [55] have analyzed the aperture coupled DRA using MOM method. Borowiec et al. [56] have used MOM approach for analyzing a cavity backed, slot excited DRA. Abdulla and Chakraborty [57] have analyzed hemispherical DRA excited with a thick slot at the short circuited end of waveguide using MM method. For a hemispherical DRA, the integral of the admittance matrix corresponding to the homogeneous Green's function has been evaluated by expressing the homogeneous Green's function in terms of a double summation using MM method [58]. Broad wall longitudinal slot coupled hemispherical DRA has been analyzed using MOM [59]. Thus, the moment method has been successfully applied on several cases of DRAs. Thus, several cases of DRAs have been resolved using moment method in this section.

5. Modeling of DRAs using FEM

Engineering domain is one of vastest system, where mathematical model is one of the suitable alternative for describing the behavior of the whole system in a constructive manner. Finite

element method is one of those mathematical modeling technique, initially used for structural analysis during 1960–1970s. However its introduction with electromagnetic scattering problems in 1980s is well documented in [60]. Initially it was mainly based on static, quasi-static, and guided wave problems. In course of time this was highly appreciated for microwave and millimeter-wave system optimization as well as for EM radiation means for antenna. In addition to this, the finite element method (FEM) is one of the numerical tool to have the approximate solution which can be used in general purpose computers and thus increased the usability. In FEM, mainly the problems are divided into different sub domains, known as finite element which causes the problem to have many number of finite element patches [61], and in context to this, now this method is considered to be one of the finest method in computational electromagnetics mainly for antenna modeling, with evidence of good number of publications in electromagnetic domain. However the basic steps of modeling of dielectric resonator antenna (three dimensional structure), is discussed in this section.

5.1. Few general steps for FEM implementation on DRAs

The procedure of implementing FEM for modeling of a dielectric resonator antenna is quite different than those for microstrip patch antennas. The way of defining discretization of the finite volume as well as the boundary condition is quite important in FEM modeling. For smooth understanding, the basic approaches of FEM in context of DRA modeling some basic mathematical steps are elaborated here.

5.2. Step 1: formulation of basic fields

For any electromagnetic problem, first we need to define the field. As here DR-antenna is a three dimensional structure, so let us assume a three-dimensional scattering problem as shown in **Figure 4(a)**, having finite volume V with of permittivity ε and permeability μ surrounded by an area of volume V_∞ of permittivity ε_0 and permeability μ_0 at a finite distance of S. When electromagnetic wave input having angular frequency (ω) is applied then it starts scattering. The electromagnetic filed inside the volume V (E_1, H_1) and outside volume V (E_2, H_2) can be written in terms of vector differential wave equations for a source free region [62].

(a)   (b)
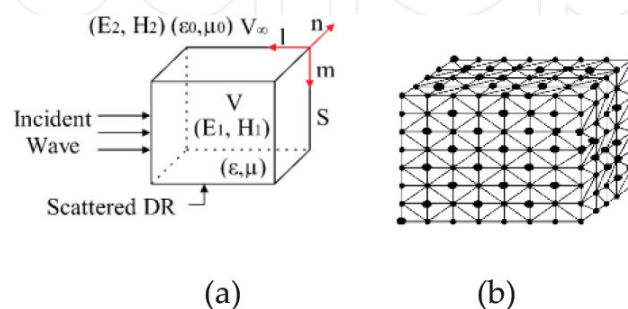
Figure 4. (a) Scattering problem of DRA [62] and (b) discretization of the DR structure [63].

$$\nabla \times \frac{1}{\mu} \nabla \times \overline{E_1} - \omega^2 \varepsilon \overline{E_1} = 0 \tag{32}$$

$$\nabla \times \frac{1}{\varepsilon} \nabla \times \overline{H_1} - \omega^2 \mu \overline{H_1} = 0 \tag{33}$$

$$\nabla \times \nabla \times \overline{E_2} - k_0^2 \overline{E_2} = 0 \tag{34}$$

$$\nabla \times \nabla \times \overline{H_2} - k_0^2 \overline{H_2} = 0 \tag{35}$$

Where K = Free space wave number.

Here three-dimensional FEM can be applied for the solution of fields inside the volume V, whereas a surface integral equation (which is a solution for the fields in V_∞) is then applied to provide a necessary boundary constraint on the surface for the finite element solution. Now, it is the task to solve Eqs. (32) and (33) which is inside the volume, using three-dimensional FEM.

In context of this, the corresponding functional of Eqs. (32) and (33) is highly desired. With little mathematics (using vector identity and applying divergence theorem) the corresponding functional of Eqs. (32) and (33) for the entire domain $V + V_\infty$ can be written as [63]:

$$F = \frac{1}{2} \iiint_V \left[\frac{1}{\omega^2 \mu} (\nabla \times \overline{E_1}) \cdot (\nabla \times \overline{E_1}) - \varepsilon \overline{E_1} \cdot \overline{E_1} \right] dV + \frac{1}{2} \iint_S \frac{1}{\omega^2 \mu} \left[(\nabla \times \overline{E_1}) \times \overline{E_1} \right] \cdot \hat{n} dS \tag{36}$$

$$F = \frac{1}{2} \iiint_V \left[\frac{1}{\omega^2 \varepsilon} (\nabla \times \overline{H_1}) \cdot (\nabla \times \overline{H_1}) - \varepsilon \overline{H_1} \cdot \overline{H_1} \right] dV + \frac{1}{2} \iint_S \frac{1}{\omega^2 \varepsilon} \left[(\nabla \times \overline{H_1}) \times \overline{H_1} \right] \cdot \hat{n} dS \tag{37}$$

The surface integral in Eqs. (36) and (37) are nearly same and with little mathematics they can be written as:

$$\frac{j}{2\omega} \iint_S \left[(\overline{E_1} \times \overline{H_1}) \right] \cdot \hat{n} dS \tag{38}$$

Further, in scalar form Eqs. (36) and (37) can be rewritten as:

$$F = \frac{1}{2} \iiint_V \left\{ \frac{1}{\omega^2 \mu} \left[\left(\frac{\partial E_z}{\partial y} - \frac{\partial E_y}{\partial z} \right)^2 + \left(\frac{\partial E_x}{\partial z} - \frac{\partial E_z}{\partial x} \right)^2 + \left(\frac{\partial E_y}{\partial x} - \frac{\partial E_x}{\partial y} \right)^2 \right] - \varepsilon \left[E_x^2 + E_y^2 + E_z^2 \right] \right\} dV$$

$$+ \frac{j}{2\omega} \iint_S (E_l H_m - E_m H_l) dS$$

$$\tag{39}$$

$$F = \frac{1}{2} \iiint_V \left\{ \frac{1}{\omega^2 \varepsilon} \left[\left(\frac{\partial H_z}{\partial y} - \frac{\partial H_y}{\partial z} \right)^2 + \left(\frac{\partial H_x}{\partial z} - \frac{\partial H_z}{\partial x} \right)^2 + \left(\frac{\partial H_y}{\partial x} - \frac{\partial H_x}{\partial y} \right)^2 \right] - \mu \left[H_x^2 + H_y^2 + H_z^2 \right] \right\} dV$$

$$+ \frac{j}{2\omega} \iint_S (E_l H_m - E_m H_l) dS$$

$$\tag{40}$$

Here, the subscript 1 on both E and H has been dropped for convince. Also, *l* and *m* are two orthogonal unit vectors tangential to the surface S and they are so oriented that (*l*, *m*, *n*) form a right handed systems.

5.3. Step 2: finite element discretization and surface integral formulation for fields

The finite volume V of the DR can be subdivided into numbers of three-dimensional elements which can be either tetrahedral, rectangular prisms, or a triangular prisms or even better isotropic elements [63] (as shown in **Figure 4(b)**) that depends upon the applications and geometry type. However, within each element the field can be expressed as;

$$\overline{E}^e = \sum_{i=1}^{n} N_i^e(x,y,z)\overline{E}_i^e \text{ and } \overline{H}^e = \sum_{i=1}^{n} N_i^e(x,y,z)\overline{H}_i^e \tag{41}$$

Here; n is the number of nodes, N_i^e is the interpolation function, and $\overline{E}_i^e$, $\overline{H}_i^e$ in the fields at the ith node.

Substituting Eq. (41) into Eq. (39) or Eq. (40) and applying Rayleigh-Ritz procedure the system of liner equations can be obtained [62]. Now applying three-dimensional finite element discretization to Eq. (39) results in the matrix equation;

$$\left[\overline{\overline{K}}_{ll}\right] \cdot \{\overline{E}_l\} + \left[\overline{\overline{K}}_{lS}\right] \cdot \{\overline{E}_S\} = 0 \tag{42}$$

and

$$\left[\overline{\overline{K}}_{ll}\right] \cdot \{\overline{E}_{ll}\} + \left[\overline{\overline{K}}_{SS}\right] \cdot \{\overline{E}_S\} + \left[\overline{\overline{K}}_{SS}'\right] \cdot \{\overline{H}_S\} = 0 \tag{43}$$

where $\overline{E}_l$ is the electric field nodes interior to the surface S; $\overline{E}_S$ is the tangential electric field at the nodes on S; $\overline{H}_S$ is the tangential magnetic field at the nodes on S, $\overline{\overline{K}}$ is the matrix having three dimensions.

In close observation to Eqs. (41) and (42), it is clear that, they do not form a complete system and this can be achieved by developing matrix equation relating to $\{\overline{E}_S\}$ and $\{\overline{H}_S\}$, hence the Finite element surface integral formulation can be applied as follows:

For a finite domain V bounded by a surface S, the electric field and magnetic field inside, in the form of incident electric field can be expressed as [62]:

$$\overline{E}(\overline{R}) = \overline{E}^{INC}(\overline{R}) - \iint_S \left\{ \nabla \times \overline{\overline{G}}_0\left(\overline{R},\overline{R}'\right) \cdot \left[\hat{n}' \times \overline{E}\left(\overline{R}'\right)\right] - j\omega\mu\overline{\overline{G}}_0\left(\overline{R},\overline{R}'\right) \cdot \left[\hat{n}' \times \overline{H}\left(\overline{R}'\right)\right] \right\} dS' \tag{44}$$

After discretizing the above equation on the surface S, a matrix equation comes in the form:

$$\left[\overline{\overline{B}}_{SS}\right] \cdot \{\overline{E}_S\} + \left[\overline{\overline{B}}_{SS}'\right] \cdot \{\overline{H}_S\} = \left\{\overline{E}_S^{INC}\right\} \tag{45}$$

where $\overline{E}_S^{INC}$ is the tangential incident electric field at the node on S, and again $\overline{\overline{B}}$ denotes a matrix of three dimensions. Now the combination of Eqs. (42), (43), and (45) form a complete system in order to solve the nodal fields.

For modeling of DRAs, these basic steps of FEM method has also been utilized but the referenced literature on it is very much limited. However some of the collected articles are discussed here. Fargeot et al. [64] have used DR antenna with a non-destructive method based on FEM for characterizing material. A microstrip-coupled cylindrical DRA excited in the $HE_{11\delta}$ mode has been investigated theoretically as well as experimentally using FEM [65]. Neshati and Wu [66] have proposed a microstrip-slot coupled rectangular DRA using FEM. A probe fed rectangular DRA supported by finite ground plane and operated in TE_{111} mode has been analyzed numerically using FEM method [67]. Analysis of waveguide fed DRA has been carried out using FEM [68].

6. Hybrid numerical methods for DRAs modeling

The basic steps for FDTD, MoM, and FEM have well discussed in previous sections. However, in this section several cases of DRAs modeling have been discussed using a combination of more than one numerical method like: combination of MOM with others methods and the combination of FEM with others methods, respectively.

The moment method (MM) has been combined with FDTD for analyzing a rectangular DRA over a finite ground plane with microstrip slot excitation [69] and for analyzing a DRA fed by a microstrip line coupled with DR through a narrow aperture in a ground plane [70], respectively. Again, the moment method has been combined with mode matching method for studying the scattering problem of the probe-fed hemispherical DR antenna utilizing a conducting conformal strip excitation operated in the fundamental TE_{111} mode [71]. A new excitation scheme employing a conducting conformal strip has been analyzed for DRA excitation operated in fundamental mode TE_{111} using mode-matching method [72].

Few cases of DRAs have also been modeled using a combination of FEM and other numerical methods, which are discussed here. The hybrid combination of FEM and conventional dielectric waveguide model (CDWM) has been used for studying a probe-fed rectangular DRA supported by a ground plane theoretically and experimentally, simultaneously [73]. The FEM has again been combined with finite integral method (FIT) for analyzing a novel "C"-shaped DRA [74] as well for reducing the mutual coupling between two identical cylindrical DRAs [75] mounted on a conducting hollow circular cylindrical structure in E-plane and H-plane coupling, respectively. A reflectarray mounted on or embedded in cylindrical and spherical surfaces has been analyzed using finite integration method and transmission line method at 11.5 GHz for satellite applications [76]. Again Dhouib et al. [77] have reported the analysis of aperture-coupled and microstrip proximity coupled DRAs using transmission line method. A hybrid combination of FEM and finite integration method (FIT) has also been used for analyzing an electrically small and high permittivity "C" DRA [78]. The FEM has been combined with FDTD for designing multi-segment DRA [79] and for structural mechanics analysis of DRAs [80], respectively.

7. Electron paramagnetic resonance resonator types and effects

In general electron paramagnetic resonance (EPR) is a spectroscopy tool used in different emerging areas of physics, chemistry, and biology for the characterization of paramagnetic species [81–83]. In general there are some specific types of EPR resonators, say wave-guide resonator, microstrip resonator, dielectric resonator, and transmission line resonator [83]. Unlike traditional EPR wave-guide cavities operating in the transverse electric TE mode, on which both longitudinal and transverse dimensions scale with frequency, transmission-line resonators operating in the transverse electromagnetic (TEM) mode have their resonant frequency set only by the longitudinal dimension and the effective relative permittivity of the medium (εref) which ultimately results in shorter transverse dimensions than half wavelength [84]. As per [85] the conventional EPR systems i.e. using wave guide cavities as well inductive detection have a sensitivity limitation to near 10^{11} spins/GHz$^{1/2}$, which is inadequate for studying samples having smaller number of spins. On the other hand if we see, dielectric resonators (DR) which are made of a single crystal/ceramic material with comparatively high dielectric constants with low loss have better sensitivity of EPR than those conventional ones. It can also achieve sensitivity nearly 5×10^{8} spins/G [85]. Apart from this, the small size of the DR also helps in using it as the central part of mini-EPR, while the absence of background signals gives more degrees of freedom for precise recordings of EPR spectra. As per [85] different kind of shapes can be actualized in a DR in order to store and analyze samples. It can be noted that more no of shapes helps in storing and analyzing more number of samples simultaneously. However the modeling work of making different types of shapes as well as their effect on resonator characteristics can be well developed by the numerical methods discussed in previous sections.

Author details

Sounik Kiran Kumar Dash[1] and Taimoor Khan[2]*

*Address all correspondence to: ktaimoor@gmail.com

1 CHRIST (Deemed to be University), Bengaluru, Karnataka, India

2 National Institute of Technology Silchar, Silchar, Assam, India

References

[1] Richtmyer RD. Dielectric resonators. Journal of Applied Physics. Jun. 1939;**10**:391-398

[2] Long SA, Mcallister MW, Shen LC. The resonant cylindrical dielectric cavity antenna. IEEE Transactions on Antennas and Propagation. May 1983;**31**(3):406-412

[3] Mongia RK, Bhartia P. Dielectric resonator antennas—A review and general design relations for resonant frequency and bandwidth. International Journal of Microwave and Millimeter-Wave Computer-Aided Engineering. Jul. 1994;**4**(3):230-247

[4] Dash SKK, Khan T, De A. Modelling of dielectric resonator antennas using numerical methods: A review. Journal of Microwave Power and Electromagnetic Energy. 2016;**50**(4): 269-293

[5] Yee KS. Numerical solution of boundary value problems involving Maxwell's equation in isotropic media. IEEE Transactions on Antennas and Propagation. 1966;**14**:302-307

[6] Inan US, Marshall RA. Numerical Electromagnetics: The FDTD Method. Cambridge: Cambridge University Press; 2011

[7] Kumar AVP. Development of a novel wideband cylindrical dielectric resonator antenna [PhD dissertation]. Cochin, India: Dept. of Electronics, Cochin Univ. of Science and Tech; 2008 Jan

[8] Mur G. Absorbing boundary condition for the finite-difference approximation of the time-domain electromagnetic field equations. IEEE Transactions on Electromagnetic Compatibility. 1981;**23**:377-382

[9] Berenger JP. A perfectly matched layer for the absorption of electromagnetic waves. Journal of Computational Physics. 1994;**114**:185-200

[10] Shum SM, Luk KM. Characteristics of dielectric ring resonator antenna with an air gap. IET Electronics Letters. Feb. 1994;**30**(4):277-278

[11] Shum SM, Luk KM. Numerical study of a cylindrical dielectric-resonator antenna coated with a dielectric layer. IEEE Transactions on Antennas and Propagation. Apr. 1995;**142**(2): 189-191

[12] Shum SM, Luk KM. FDTD analysis of probe-fed cylindrical dielectric resonator operating in fundamental broadside mode. IET Electronics Letters. Jul. 1995;**31**(15):1210-1212

[13] Shum SM, Luk KM. FDTD analysis of probe-fed cylindrical dielectric resonator antenna. IEEE Transactions on Antennas and Propagation. Mar. 1998;**46**(3):325-333

[14] Twu Chen H, Cheng YT, Ke SY. Probe-fed section-spherical dielectric resonator antennas. In: Proceedings of the IEEE Asia Pacific Microwave Conference, vol. 2. Nov. 1999. pp. 359-362

[15] Guo YX, Luk KM, Leung KW. Mutual coupling between rectangular dielectric resonator antennas by FDTD. IEE Proceedings—Microwaves, Antennas and Propagation. Aug. 1999;**146**(4):292-294

[16] Guo YX, Luk KM, Leung KW. Characteristics of aperture-coupled cylindrical dielectric resonator antennas on a thick ground plane. IEE Proceedings—Microwaves, Antennas and Propagation. Dec. 1999;**146**(6):439-442

[17] Farahat N, Yul W, Mittra R, Koleck T. Cross-shaped dielectric resonator antenna analysis using the conformal finite difference time domain (CFDTD) method. In: Proc. IEEE Antennas and Propagation Society Int. Sym, vol. 3; Boston, MA, USA. Jul. 2001. pp. 549-552

[18] Kamchouchi HE, EI-Kayar YG. Finite difference time domain solutions for the dielectric resonator antenna problems with different feeding signals. In: Proc. IEEE 18th Nat. Radio Science Conf; Mansoura. Mar. 2001. pp. 63-70

[19] Semouchkina E, Semouchkin G, Caol W, Mittra R. FDTD analysis of modal characteristics of dielectric resonator antennas. In: Proc. IEEE Antennas and Propagation Society Int. Sym. Vol. 4. 2002. pp. 466-469

[20] Gentili GB, Morini M, Selleri S. Relevance of coupling effects on DRA array design. IEEE Transactions on Antennas and Propagation. Mar. 2003;**51**(3):399-405

[21] Neshati MH, Wu Z. Microstrip-slot coupled rectangular dielectric resonator antenna: Theoretical modelling & experiments. In: Proc. IET 12th Int. Conf. on Antennas and Propagation; March 2003, Conf. Pub. No. 491. Vol. 2. pp. 759-762

[22] Paran K, Kamyab M, Tabatabaei NA. FDTD analysis of top-hat monopole antennas loaded with radially layered dielectric. International Journal of Engineering-Transactions A: Basics. 2004;**17**(3):251-262

[23] Zhang Y, Kishk AA, Yakovlev AB, Glisson AW. FDTD analysis of a probe-fed dielectric resonator antenna in rectangular waveguide. In: Proc. IEEE/ACES Int. Conf. on Wireless Communications and Applied Computational Electromagnetics. Apr. 2005. pp. 371-375

[24] EI-Deen E, Zainud-Deen SH, Sharshar HA, Binyamin MA. The effect of the ground plane shape on the characteristics of rectangular dielectric resonator antennas. In: Proc. IEEE Antennas and Propagation Society Int. Sym; Albuquerque, NM. Jul. 2006. pp. 3013-3016

[25] Nomura T, Sato K. Topology design optimization of dielectric resonator antennas using finite-difference time-domain method. In: Proc. IEEE Antennas and Propagation Society Int. Sym; Albuquerque, NM. Jul. 2006. pp. 1317-1320

[26] Mohanana P, Mridula S, Paul B, Suma MN, Bijumon PV, Sebastian MT. FDTD analysis of rectangular dielectric resonator antenna. Journal of the European Ceramic Society. 2007;**27** (8–9):2753-2757

[27] Zainud-Deen SH, EI-Doda SI, Awadalla KH, Sharshar HA. The relation between lumped-element circuit models for cylindrical dielectric resonator and antenna parameters using MBPE. Progress in Electromagnetics Research. 2008;**1**:79-93

[28] Li A, Leung KW, Sheng XQ. Differentially fed rectangular dielectric resonator antenna. In: Proc. IEEE Global Symp. on Millimeter Waves; Nanjing. Apr. 2008. pp. 157-160

[29] Li B, Leung KW. On the differentially fed rectangular dielectric resonator antenna. IEEE Transactions on Antennas and Propagation. Feb. 2008;**56**(2):353-359

[30] Yao B, Zheng Q, Peng J, Zhong R, Li S, Xiang T. An efficient 2-D FDTD method for analysis of parallel-plate dielectric resonators. IEEE Antennas and Wireless Propagation Letters. Aug. 2011;**10**:866-868

[31] Ganguly D, Das S, Rojatkar A, Guha D. Ultra-wideband pawn DRA: Time domain studies. In: Proc. IEEE Indian Antenna Week; Kolkata. Dec. 2011. pp. 1-4

[32] Dzulkipli NI, Jamaluddin MH, Gillard R, Sauleau R, Ngah R, Kamarudin MR, et al. Mutual coupling analysis using FDTD for di- electric resonator antenna reflectarray radiation prediction. Progress in Electromagnetics Research B. 2012;**41**:121-136

[33] Gupta A, Gangwar RK. Analysis of conformal strip feed triangular dielectric resonator antenna using FDTD method. In: Proc. IEEE Int. Conf. on Computational Electromagnetics; Hong Kong. Feb. 2015. pp. 92-94

[34] Harrington RF. Field Computation by Moment Methods. Malabar, FL: Krieger; 1968

[35] Harrington RF. Matrix methods for field problems. Proceedings of the IEEE. 1967;**55**: 136-149

[36] Harrington RF. Time Harmonic Electromagnetic Fields. New York: McGraw-Hill; 1961

[37] Ng HK. Rigorous analysis of the hemispherical dielectric resonator antenna with a parasitic patch [PhD dissertation]. Hong Kong: Dept. of Electronics Engg. City Univ; Oct 2003

[38] Leung KW, Ng HK. Dielectric resonator antenna fed by displaced conformal strip. Microwave and Optical Technology Letters. 2001;**29**:185-187

[39] Kishk AA, Zunoubi MR. Analysis of the dielectric disc antennas above a grounded dielectric substrate. In: Proc. IEEE Antennas and Propagation Society Int. Symp. Dig; Chicago, IL, USA. Jun 1992. pp. 2171-2174

[40] Junker JP, Kishk AA, Glisson AW. Input impedance of an aperture coupled dielectric resonator antenna. In: Proc. IEEE Antennas and Propagation Society Int. Symp. Dig; Seattle, WA, USA. Jun 1994. pp. 748-751

[41] Leung KW, Luk KM. Moment method solution of aperture-coupled hemispherical dielectric resonator antenna. In: Proc. IEEE Antennas and Propagation Society Int. Symp. Dig., vol. 2; Seattle, WA, USA. Jun. 1994. pp. 752-755

[42] Leung KW, Luk KM. Moment method solution of aperture-coupled hemispherical dielectric resonator antenna using exact modal Green's function. IEE Proceedings - Microwaves, Antennas and Propagation. Oct. 1994;**141**(5):377-381

[43] Liu Z, Hewa WH, Michielssen NDE. Moment method based analysis of dielectric-resonator antennas. In: Proc. IEEE Antennas and Propagation Society Int. Symp., vol. 2; Orlando, FL, USA. Jul. 1999. pp. 806-809

[44] Chow KY, Leung KW, Luk KM, Yung EKN. Input impedance of the slot-fed dielectric resonator antenna with/without a backing cavity. IEEE Transactions on Antennas and Propagation. Feb. 2001;**49**(2):307-309

[45] Kishk A, Glisson AW, Junker GP. Bandwidth enhancement for split cylindrical dielectric resonator antenna. Progress in Electromagnetics Research. 2001;**33**:97-118

[46] Liu Z, Chew WC, Michielssen E. Numerical modeling of dielectric-resonator antennas in a complex environment using the method of moments. IEEE Transactions on Antennas and Propagation. Jan. 2002;**50**(1):79-82

[47] Chow KY, Leung KW. Cavity-backed slot-coupled dielectric resonator antenna excited by a narrow strip. IEEE Transactions on Antennas and Propagation. 2002;**50**:404-405

[48] Qian ZH, Leung KW, Chen RS. Analysis of circularly polarized dielectric resonator antenna excited by a spiral slot. Progress in Electromagnetics Research. 2004;**47**:111-121

[49] Ng HK, Leung KW. Frequency tuning of the dielectric resonator antenna using a loading disk. In: Proc. IEEE Antennas and Propagation Society Int. Symp, vol. 1. Jun. 2004. pp. 1086-1089

[50] Baghaee RM, Neshati MH, Mohassel JR. Moment method analysis of probe-fed rectangular dielectric resonator antennas with a rigorous source modeling and finite ground plane. In: Proc. IEEE Asia-Pacific Conf., vol. 5. Dec. 2005. pp. 4-7

[51] Ng HK, Leung KW. Frequency tuning of the dielectric resonator antenna using a loading cap. IEEE Transactions on Antennas and Propagation. Mar. 2005;**53**(3):1229-1232

[52] Eshrah IA, Kishk AA, Yakovlev AB, Glisson AW. Theory and implementation of dielectric resonator antenna excited by a waveguide slot. IEEE Transactions on Antennas and Propagation. Jan. 2005;**53**(1):483-494

[53] Leung KW, So KK. Analysis of the coaxial-aperture-fed dielectric resonator antenna. In: Proc. IEEE Antennas and Propagation Society Int. Symp.; Albuquerque, NM. Jul. 2006. pp. 2503-2506

[54] Lam HY, Leung KW. Analysis of U-slot-excited dielectric resonator antennas with a backing cavity. IEE Proceedings - Microwaves, Antennas and Propagation. Oct. 2006; **153**(5):480-482

[55] Ge Y, Esselle KP. The analysis of a rectangular dielectric resonator antenna using the method of moments. In: Proc. IEEE Antennas and Propagation Society Int. Symp.; Salt Lake City, UT, USA. Vol. 3. Jul. 2000. pp. 1454-1457

[56] Borowiec R, Kucharski AA, Slobodzian PM. Slot excited dielectric resonator antenna above a cavity - Analysis and experiment. In: Proc. IEEE Int. Conf. on Microwaves, Radar & Wireless Communications; Krakow. May 2006. pp. 824-827

[57] Abdulla P, Chakraborty A. Rectangular waveguide-fed hemispherical dielectric resonator antenna. Progress in Electromagnetics Research. 2008;**83**:225-244

[58] Kakade AB, Ghosh B. Efficient technique for the analysis of microstrip slot coupled hemispherical dielectric resonator antenna. IEEE Antennas and Wireless Propagation Letters. 2008;**7**:332-336

[59] Abdulla P, Singh YK, Chakraborty A. Theoretical and experimental study on broad wall slot coupled dielectric resonator antennas. In: Proc. IEEE Asia Pacific Microwave Conf.; Singapore. Dec. 2009. pp. 2750-2753

[60] Jin JM. The Finite Element Method in Electromagnetics. New York: John Wiley & Sons Inc; 1993

[61] Kwon YW, Bang HC. The Finite Element Method Using MATLAB. New York: CRC Press; 1997. ISBN 0-8493-9653-0

[62] Jin J, Liepa VV, Volakis JL. Finite Element Methods for Electromagnetic Scattering. Ann Arbor, MI: Radiation Lab., Dept. of Elect Eng and Comp Science, The Univ. of Michigan; 1989 Oct. p. 868

[63] Zienkiewicz OC, Taylor RL, Zhu JZ. The Finite Element Method: Its Basis and Fundamentals. Burlington, MA: Elsevier Butterworth-Heinemann; 2005

[64] Fargeot S, Julien-Vergonjanne A, Guillon P. Dielectric resonator antenna for material characterization. In: Proc. IEEE Conf. on Precision Electromagnetic Measurements Dig; Braunschweig, Germany. Jun. 1996. pp. 70-71

[65] Drossos G, Wu Z, Davis LE. Theoretical and experimental investigations on a microstrip-coupled cylindrical dielectric resonator antenna. Microwave and Optical Technology Letters. Apr. 1999;**21**(1):18-25

[66] Neshati MH, Wu Z. Finite element analysis & experimental studies of microstrip slot coupled rectangular dielectric resonator antenna. In: Proc. IEEE Int. Conf. on Microwave and Millimeter Wave Technology. Aug. 2004. pp. 118-121

[67] Neshati MH, Wu Z. Numerical modeling and experimental study of probe-fed rectangular dielectric resonator antenna (RDRA) supported by finite circular ground plane. International Journal of Engineering-Transactions A: Basics. Sept. 2004;**17**(3):269-280

[68] Sheng XQ, Leung KW, Yung EKN. Analysis of waveguide-fed dielectric resonator antenna using a hybrid finite element method/moment method. IEE Proceedings - Microwaves, Antennas and Propagation. Feb. 2004;**151**(1):91-95

[69] Shin J, Kishk AA, Glisson AW. Analysis of rectangular dielectric resonator antennas excited through a slot over a finite ground plane. In: Proc. IEEE Antennas and Propagation Society Int. Symp; Salt Lake City, UT, USA. Vol. 4. Jul. 2000. pp. 2076-2079

[70] Ge Y, Esselle KP. Microwave dielectric-resonator antenna analysis and design. In: Proc. IEEE Asia Pacific Microwave Conf; Sydney, NSW. Dec. 2000. pp. 1473-1476

[71] Chen ZN, Leung KW, Luk KM, Yung EKN. Electromagnetic scattering from the probe-fed hemispherical dielectric resonator antenna. In: Proc. IEEE Antennas and Propagation Society Int. Symp. Dig., vol. 2; Baltimore, MD, USA. Jul. 1996. pp. 1410-1413

[72] Leung KW. Conformal strip excitation of dielectric resonator antenna. IEEE Transactions on Antennas and Propagation. Jun. 2000;**48**(6):961-967

[73] Neshati MH, Wu Z. Rectangular dielectric resonator antennas: Theoretical modelling and experiments. In: Proc. IEE Int. Conf. on Antennas and Propagation, vol. 2; Manchester. Apr. 2001. pp. 866-870

[74] Rotaru MD, Sykulski JK. Design and analysis of a novel compact high permittivity dielectric resonator antenna. IEEE Transactions on Magnetics. Mar. 2009;**45**(3):1052-1055

[75] Zainud-Deen SH, Malhat HA, Awadalla KH. Reduction of mutual coupling between two dielectric resonator antennas mounted on a circular cylindrical ground plane. In: Proc. IEEE Antennas and Propagation Society Int. Symp.; Toronto, ON. Jul. 2010. pp. 1-4

[76] Zainud-Deen SH, EI-Shalaby NA, Malhat HA, Gaber SM, Awadalla KH. Dielectric resonator antenna reflector—Rays mounted on or embedded in conformal surfaces. Progress in Electromagnetics Research C. 2013;**38**:115-128

[77] Dhouib A, Stubbs MG, Mongia RK, Lecours M. TLM analysis of rectangular dielectric resonator antennas. In: Proc. IEEE Antennas and Propagation Society Int. Symp. Dig., vol 1; Newport Beach, CA, USA. Jun. 1995. pp. 782-785

[78] Rotaru M, Sykulski JK. Numerical investigation on compact multimode dielectric resonator antennas of very high permittivity. IET Science, Measurement and Technology. May 2009;**3**(3):217-228

[79] Rashidian A, Forooraghi K, Tayefeh MR. Design algorithm of multi-segment dielectric resonator antennas (MSDRAs). In: Proc. IEEE Int. Conf. on Microwave and Millimeter Wave Technology. Aug. 2004. pp. 134-137

[80] Nomura T, Sato K, Nishiwaki S, Yoshimura M. Topology optimization of multiband dielectric resonator antennas using finite-difference time-domain method. In: Proc. IEEE International Workshop on Antenna Technology: Small and Smart Antennas Metamaterials and Applications; Cambridge. Mar. 2007. pp. 147-150

[81] Geifman IN, Golovina IS. Electromagnetic characterization of rectangular ferroelectric resonators. Journal of Magnetic Resonance. 2005;**174**:292

[82] Geifman IN, Golovina IS. Optimization of ferroelectric resonators for enhanced EPR sensitivity. Concepts in Magenetic Resonance. 2005;**26B**:46

[83] Golovina I, Geifman I, Belous A. New ceramic EPR resonators with high dielectric permittivity. Journal of Magnetic Resonance. 2008;**195**:52

[84] Torrezan AC, Mayer Alegre TP, Medeiros-Ribeiro G. Microstrip resonators for electron paramagnetic resonance experiments. Review of Scientific Instruments. 2009;**80**:044702

[85] Golovina IS, Kolesnik SP, Geifman IN, Belous AG. Novel multisample dielectric resonators for electron paramagnetic resonance spectroscopy. Review of Scientific Instruments. 2010;**81**:044702